

Organic Matrix and Solution Photochemical Studies of (Allyl)dicarbonyl(cyclopentadienyl)molybdenum Compounds

Thomas E. Bitterwolf,^{*,[a]} J. Timothy Bays,^[a] Bruce Scallorn,^[a] Callie Ann Weiss,^[a] Michael W. George,^[b] Ian G. Virrels,^[b] John C. Linehan,^[c] and Clement R. Yonker^[c]

Keywords: Photochemistry / Matrix isolation / Molybdenum / Allyl ligands

Photolysis of fresh samples of the η^3 -allyl compounds $[(\eta^5\text{-C}_5\text{H}_5)\text{Mo}(\text{CO})_2(\eta^3\text{-C}_3\text{H}_5)]$ or $[(\eta^5\text{-C}_5\text{H}_5)\text{Mo}(\text{CO})_2(\eta^3\text{-C}_3\text{H}_4\text{CH}_3)]$ in a Nujol matrix at ca. 90 K at a wavelength greater than 400 nm was found by IR spectroscopy to cause conversion of the *endo* rotamer to the *exo* rotamer. Photolysis of *exo* enriched samples of $[(\eta^5\text{-C}_5\text{H}_5)\text{Mo}(\text{CO})_2(\eta^3\text{-C}_3\text{H}_5)]$ at wavelengths of between 360 and 400 nm reversed the photoconversion leading to an *exo* to *endo* conversion. At higher energies photochemical CO loss was also observed. In the case of the 2-methylallyl derivative, a photoproduct believed to be $[(\eta^5\text{-C}_5\text{H}_5)\text{Mo}(\text{H})(\text{CO})(\eta^4\text{-C}_4\text{H}_6)]$ was observed

along with CO loss. Time-resolved IR studies of the flash photolysis of $[(\eta^5\text{-C}_5\text{H}_5)\text{Mo}(\text{CO})_2(\eta^3\text{-C}_3\text{H}_5)]$ in *n*-heptane confirm both *endo* to *exo* rotamer conversion and CO loss. Under these conditions, the species formed after CO loss is probably $[(\eta^5\text{-C}_5\text{H}_5)\text{Mo}(\text{CO})(n\text{-heptane})(\eta^3\text{-C}_3\text{H}_5)]$. When $[(\eta^5\text{-C}_5\text{H}_5)\text{Mo}(\text{CO})_2(\eta^3\text{-C}_3\text{H}_5)]$ was dissolved in supercritical ethylene and photolyzed, $[(\eta^5\text{-C}_5\text{H}_5)\text{Mo}(\text{CO})(\text{C}_2\text{H}_4)(\eta^3\text{-C}_3\text{H}_5)]$ was formed. A mechanism involving two distinct excited states is proposed to account for the photoreversible *endo/exo* transformations.

Introduction

In 1963 Cousins and Green^[1] reported the synthesis of $[(\eta^5\text{-C}_5\text{H}_5)\text{Mo}(\text{CO})_3(\eta^1\text{-C}_3\text{H}_5)]$ (**1**) and $[(\eta^5\text{-C}_5\text{H}_5)\text{Mo}(\text{CO})_2(\eta^3\text{-C}_3\text{H}_5)]$ (**2**) by reaction of $[(\eta^5\text{-C}_5\text{H}_5)\text{Mo}(\text{CO})_3]^-$ with allyl chloride. Compound **2** could also be efficiently formed from **1** by photolysis with ultraviolet radiation. Several years after the initial discovery, King noted that **2** appeared to exist in solution as two species.^[2] Davidson,^[3] Faller^[4] and their co-workers correctly established the structures of the two conformers to be the *endo* and *exo* rotamers shown in Figure 1 with an *exo/endo* ratio of 3:1 in benzene. Introduction of a methyl group into the 2-position on the allyl group in **3** reverses the orientational preference so that the *endo* rotamer becomes strongly favored. Curiously absent in this early literature were comments concerning thermal or photochemical substitution of the carbonyl groups in **2** or **3**.

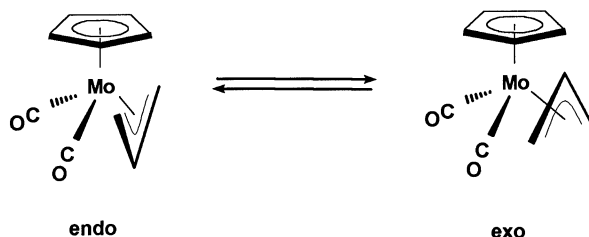
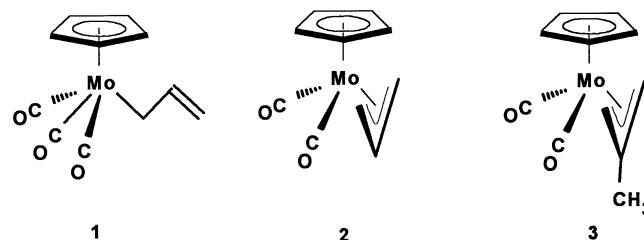


Figure 1. *endo/exo* equilibrium of $[(\eta^5\text{-C}_5\text{H}_5)\text{Mo}(\text{CO})_2(\eta^3\text{-C}_3\text{H}_5)]$



As part of our ongoing studies on the photochemistry of organometallic compounds, we have examined the photolysis of **1**, **2**, and **3** in Nujol and 2-methyltetrahydrofuran (MeTHF) glass matrices at 90 K. These studies have revealed a previously unknown photochemically driven rotation of the η^3 -allyl group, as well as other haptotropic transformations. Time-resolved IR studies and photochemical reactions in supercritical ethylene have been carried out to provide additional evidence for the observed intermediates. We have previously reported Nujol matrix studies of molybdenum and chromium compounds in which a pendant η^3 -cyclopentenyl ring was attached to the cyclopentadienyl ring.^[5] A brief study of the photochemistry of the tungsten analog of **1** in a methane matrix has been reported by Rest.^[6] The results of the present study along with those of Limberg et al.^[7] on the photolysis of **1** in a frozen argon matrix reported in this issue, shed new light on the interpretation of the earlier spectroscopic data.

Results and Discussion

Organic Matrix Photochemistry

Compounds **1**, **2** and **3** were prepared by standard literature procedures.^[8] Nujol matrix studies were carried out us-

^[a] Department of Chemistry, University of Idaho
Moscow, ID 83844-2343, USA
E-mail: bitterte@uidaho.edu

^[b] Department of Chemistry, University of Nottingham
Nottingham NG7 2RD, UK

^[c] Chemical Sciences Department, Pacific Northwest National Laboratory,
P. O. Box 999, Richland, WA 99352, USA

ing a cryostat developed by Rest and procedures as previously described.^[9] MeTHF glass matrix studies were carried out using a Specac Model 21525 Variable Temperature Cell.

The electronic spectrum of **2** has a strong absorption band below 290 nm that is probably associated with a metal-to-ligand charge-transfer band. A medium intensity band is observed at 345 nm with a shoulder at about 400 nm. At high concentrations of **2**, a tail of these visible bands can be seen to extend as high as 600 nm.

A Nujol solution of **2** was frozen to ca. 90 K and the IR spectrum recorded as shown in Figure 2a. IR data for all compounds are presented in Table 1. IR bands for both the *endo* (1964 and 1896 cm^{-1}) and *exo* (1955 and 1879 cm^{-1}) rotamers were found to be in an approximate 1:2 ratio. Photolysis of fresh samples at a wavelength greater than 360 nm was found by difference IR spectra to result in depletion of the *endo* rotamer bands and growth of the *exo* rotamer bands (Figure 2b). No other photochemical products were observed for photolysis at wavelengths greater than 400 nm even upon extended photolysis. When the *exo*-enriched samples formed at $\lambda_{\text{irr}} > 400$ nm were photolyzed at a wavelength between 360 and 400 nm, we were surprised to find a reversal of the photoisomerization, with conversion of the *exo* form to the *endo* form (Figure 2c). Photolysis of a fresh sample of **2** ($\lambda_{\text{irr}} = 360 \pm 10$ nm) for 3 h (Figure 2d) showed *endo* depletion and *exo* growth, and, in addition, produced a small band at 2132 cm^{-1} and a broad feature at 1843 cm^{-1} . The sample was annealed to ca. 153 K and then returned to ca. 77 K to record the IR spectrum. Under these conditions the bands at 2131 and 1843 cm^{-1} decreased while the bands of **2** increased, with the *exo* rotamer being substantially favored over the *endo* rotamer.

To further clarify the photochemical behavior of **2**, the compound was taken up in MeTHF and the solution frozen to 90 K. In this matrix the *exo* rotamer is strongly favored over the *endo* rotamer. The symmetric stretch of the *endo* isomer is detectable only as a slight asymmetry of the higher energy carbonyl stretching band, while the asymmetric *endo* band is observed as a shoulder on the lower energy band (Figure 3a). The carbonyl bands are strongly shifted ($21\text{--}30$ cm^{-1}) to lower energy in MeTHF relative to Nujol. Photolysis ($\lambda_{\text{irr}} = 450 \pm 70$ nm) resulted in bleaching of the *endo* rotamer bands at 1943 and 1864 cm^{-1} and growth of the *exo* rotamer bands at 1935 and 1851 cm^{-1} (Figure 3b). This process was reversed when the irradiation energy was increased ($\lambda_{\text{irr}} = 400 \pm 70$ nm) (Figure 3c). The small shifts of these band positions in the spectra in Figure 3 are subtraction artifacts. Higher energy photolysis ($330 < \lambda_{\text{irr}} < 400$ nm) resulted in the bands of both the *endo* and *exo* rotamers being bleached, with growth of new bands at 2031, 1816, 1789, 1744 and 1600 cm^{-1} (Figure 4a). Back photolysis of this sample ($\lambda_{\text{irr}} > 400$ nm) caused the bands at 1744 and 1600 cm^{-1} to decrease simultaneously while the bands at 1816 and 1789 cm^{-1} grew (Figure 4b). The 1789 cm^{-1} band was very weak compared to the 1816 cm^{-1} band. An *endo* to *exo* transformation was also observed upon this irradiation. It should be noted that there was no

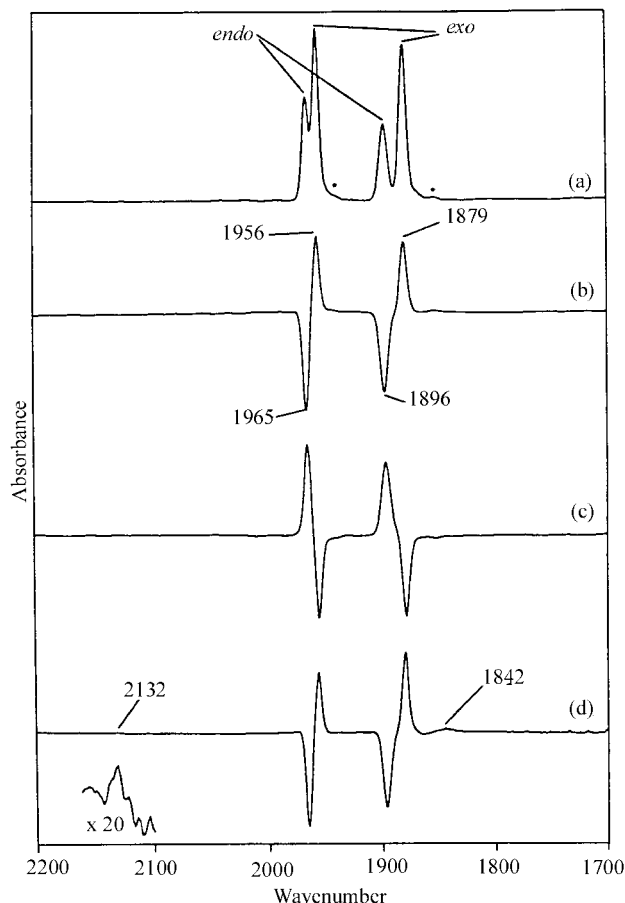


Figure 2. IR spectra of **2** isolated in a Nujol matrix: (a) starting material, ca. 90 K; (b) difference spectrum, 150 min. irradiation ($400\text{ nm} < \lambda < 470\text{ nm}$) minus starting material; (c) difference spectrum, 30 min. irradiation ($360\text{ nm} < \lambda < 450\text{ nm}$) minus 150 min. irradiation ($400\text{ nm} < \lambda < 470\text{ nm}$); (d) difference spectrum, 90 min. irradiation ($350\text{ nm} < \lambda < 370\text{ nm}$) minus starting material; bands marked with an asterisk arise from natural abundance ^{13}CO

increase or decrease of the free CO band (2131 cm^{-1}) upon back photolysis.

Compound **1** is well-known to form **2** upon photolysis. In order to further clarify the photochemical behavior of these allyl complexes, a Nujol solution of **1** contaminated with about 10% **2** was prepared. At ca. 90 K, **1** has three terminal carbonyl stretching bands at 2020, 1942, and 1931 cm^{-1} , as expected for a molecule with C_s symmetry, and a weak band at 1609 cm^{-1} associated with the unbound olefin. After photolysis ($\lambda_{\text{irr}} = 500 \pm 70$ nm) for 30 min., an IR difference spectrum demonstrated that **1** is efficiently decarbonylated ("free" CO band at 2132 cm^{-1}) and converted into both rotamers of **2** in approximately equal proportions. It is not possible to establish whether **1** preferentially forms the *endo* isomer, which then undergoes subsequent photoconversion into the *exo* isomer, or whether both *endo* and *exo* isomers are actually formed upon CO loss. Under these conditions there was no evidence for the presumed $[\text{Mo}(\text{CO})_2(\eta^1\text{-C}_3\text{H}_5)(\eta^5\text{-C}_5\text{H}_5)]$ intermediate. Again, these results parallel those observed by Limberg in a frozen Ar matrix.^[7]

Table 1. Carbonyl stretching frequencies (cm^{-1}) of allyl derivatives and their photofragments

Species	Nujol R = H, 2	MeTHF R = H, 2	Nujol R = CH_3 , 3
<i>endo</i> - $[(\eta^5\text{-C}_5\text{H}_5)\text{Mo}(\text{CO})_2(\eta^3\text{-C}_3\text{H}_4\text{R})]$	1965, 1896	1941, 1864	1960, 1888
<i>exo</i> - $[(\eta^5\text{-C}_5\text{H}_5)\text{Mo}(\text{CO})_2(\eta^3\text{-C}_3\text{H}_4\text{R})]$	1956, 1879	1935, 1850	1955, 1878
$[(\eta^5\text{-C}_5\text{H}_5)\text{Mo}(\text{CO})(\eta^3\text{-C}_3\text{H}_5)]$	1842		
$[(\eta^5\text{-C}_5\text{H}_5)\text{Mo}(\text{CO})(\text{MeTHF})(\eta^3\text{-C}_3\text{H}_5)]^{[a]}$		1816	
$[(\eta^5\text{-C}_5\text{H}_5)\text{Mo}(\text{CO})(\text{MeTHF})(\eta^3\text{-C}_3\text{H}_5)]^{[b]}$		1789	
$[(\eta^5\text{-C}_5\text{H}_5)\text{Mo}(\text{CO})(\text{MeTHF})_2(\eta^1\text{-C}_3\text{H}_5)]^{[c]}$		1745	
<i>endo</i> - $[(\eta^5\text{-C}_5\text{H}_5)\text{Mo}(\text{CO})(\eta^3\text{-C}_3\text{H}_4\text{R})]$			1868
<i>exo</i> - $[(\eta^5\text{-C}_5\text{H}_5)\text{Mo}(\text{CO})(\eta^3\text{-C}_3\text{H}_4\text{R})]$			1843
$[(\eta^5\text{-C}_5\text{H}_5)\text{Mo}(\text{CO})(\text{H})(\eta^4\text{-C}_4\text{H}_6)]$			1936

[a] Major rotamer. — [b] Minor rotamer. — [c] Free olefin band at 1600 cm^{-1} .

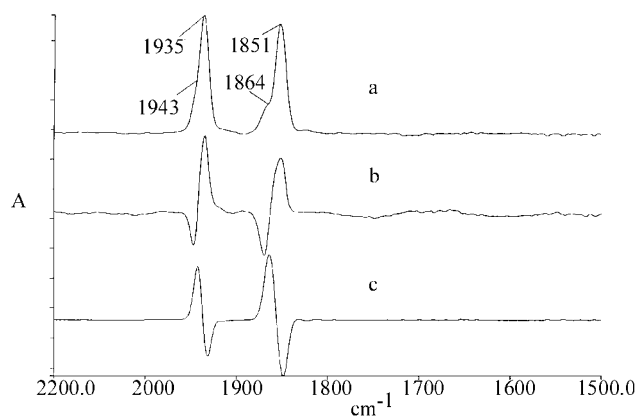


Figure 3. IR spectra of **2** isolated in a 2-methyltetrahydrofuran matrix: (a) starting material, ca. 90 K; (b) difference spectrum, 10 min. irradiation ($\lambda_{\text{irr}} = 450 \pm 70\text{ nm}$) minus starting material; (c) difference spectrum, 10 min. irradiation ($\lambda_{\text{irr}} = 400 \pm 70\text{ nm}$) minus 10 min. irradiation ($\lambda_{\text{irr}} = 450 \pm 70\text{ nm}$); the broad features around 1700 cm^{-1} are due to trace frost buildup on the cell windows

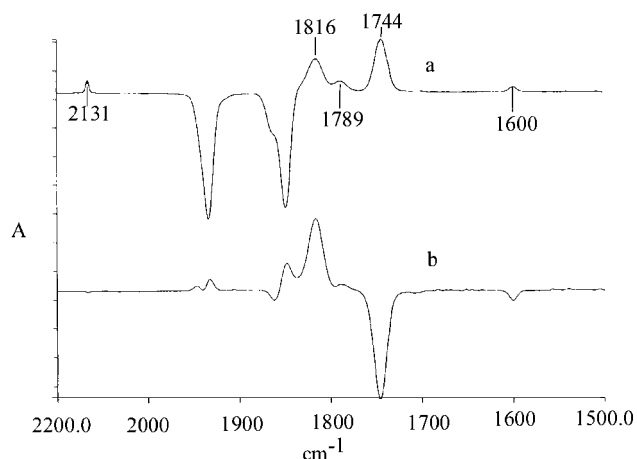
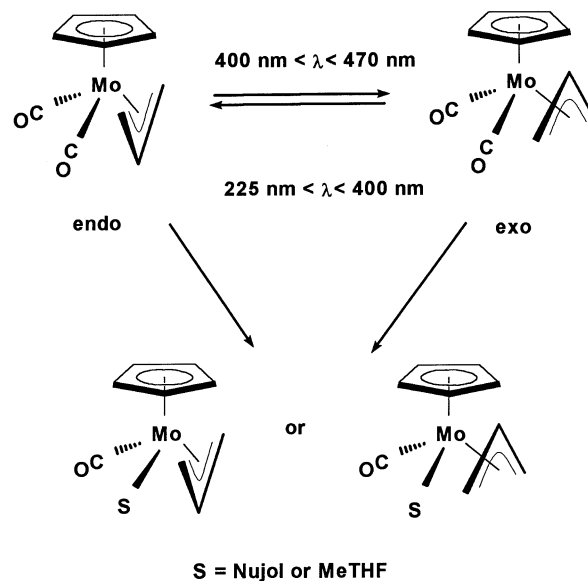


Figure 4. IR spectrum of **2** isolated in a 2-methyltetrahydrofuran matrix: (a) difference spectrum, 10 min. irradiation ($330\text{ nm} < \lambda_{\text{irr}} < 400\text{ nm}$) minus 10 min. irradiation ($\lambda_{\text{irr}} = 400 \pm 70\text{ nm}$); (b) difference spectrum 10 min. irradiation ($\lambda_{\text{irr}} > 400\text{ nm}$) minus 10 min. irradiation ($330\text{ nm} < \lambda_{\text{irr}} < 400\text{ nm}$)

Our interpretation of the observed photochemical transformations in Nujol and MeTHF is presented in Scheme 1. As also observed by Limberg in a frozen Ar matrix,^[7] the

major feature of the photolysis of **2** at longer wavelengths is the photochemical interconversion of the *endo* to the *exo* rotamers. At high energy a species formed by CO loss is observed at 1842 cm^{-1} that we assign as $[\text{Mo}(\text{CO})(\eta^3\text{-C}_3\text{H}_5)(\eta^5\text{-C}_5\text{H}_5)]$.



Scheme 1. Proposed photochemical transformations of $[(\eta^5\text{-C}_5\text{H}_5)\text{Mo}(\text{CO})_2(\eta^3\text{-C}_3\text{H}_5)]$

The donor matrix solvent MeTHF has no effect on either the low energy conversion of the *endo* rotamer to the *exo* rotamer, or on the higher energy photochemical reverse of this reaction. There was no evidence for formation of $[\text{Mo}(\text{CO})_2(\text{MeTHF})(\eta^1\text{-C}_3\text{H}_5)(\eta^5\text{-C}_5\text{H}_5)]$ under these conditions.

High energy photolysis ($\lambda_{\text{irr}} = 330\text{--}400\text{ nm}$) forms three new monocarbonyl species as well as free CO. Back photolysis bleaches the bands at 1744 and 1600 cm^{-1} and causes the bands at 1816 and 1789 cm^{-1} to grow, with no apparent gain or loss of CO. The band at 1600 cm^{-1} , consistent with a dangling η^1 -allyl group, and the single, low energy carbonyl band at 1744 cm^{-1} suggest that this species is probably $[\text{Mo}(\text{CO})(\text{MeTHF})_2(\eta^1\text{-C}_3\text{H}_5)(\eta^5\text{-C}_5\text{H}_5)]$. Back photolysis ejects an MeTHF ligand to reform the *exo* and *endo* rotamers of $[\text{Mo}(\text{CO})(\text{MeTHF})(\eta^3\text{-C}_3\text{H}_5)(\eta^5\text{-C}_5\text{H}_5)]$.

The absence of bands that might be attributable to $[\text{Mo}(\text{C}-\text{O})_2(\text{MeTHF})(\eta^1\text{-C}_3\text{H}_5)(\eta^5\text{-C}_5\text{H}_5)]$ makes it impossible to establish whether such a species is an intermediate in the formation of the observed MeTHF complexed photoproducts. The ease with which $[\text{Mo}(\text{CO})(\text{MeTHF})_2(\eta^1\text{-C}_3\text{H}_5)(\eta^5\text{-C}_5\text{H}_5)]$ is converted into $[\text{Mo}(\text{CO})(\text{MeTHF})(\eta^3\text{-C}_3\text{H}_5)(\eta^5\text{-C}_5\text{H}_5)]$ suggests that $[\text{Mo}(\text{CO})_2(\text{MeTHF})(\eta^1\text{-C}_3\text{H}_5)(\eta^5\text{-C}_5\text{H}_5)]$ might be equally sensitive to photoreversal. Rest and co-workers have reported that $[\text{Co}(\text{CO})_3(\eta^3\text{-C}_3\text{H}_5)]$ undergoes photolysis in a frozen CO matrix to give $[\text{Co}(\text{CO})_4(\eta^1\text{-C}_3\text{H}_5)]$.^[10]

Compound **3** exists almost exclusively in the *endo* form at room temperature and in Nujol at 90 K (Figure 5a), with bands at 1961 and 1888 cm^{-1} . Photolysis of **3** at long wavelengths ($\lambda_{\text{irr}} = 450 \pm 70 \text{ nm}$) results in a decrease of the bands associated with the *endo* rotamer and growth of new bands at 1955 and 1878 cm^{-1} which are assigned to the thermodynamically unfavorable, and previously unobserved, *exo* rotamer (Figure 5b). No bands at $2132 \pm 2 \text{ cm}^{-1}$ associated with “free” carbon monoxide were observed at these wavelengths. Photolysis of an *exo*-enriched sample ($330 \text{ nm} < \lambda_{\text{irr}} < 470 \text{ nm}$) (Figure 5c) results in depletion of the bands of the *exo* rotamer and growth of bands at 2131, 1961 (*endo*), 1936, 1888 (*endo*), 1866, and 1843 cm^{-1} . Continued photolysis at these wavelengths resulted in depletion of the bands of both the *exo* and *endo* rotamers and growth of the new bands. Further photolysis of this sample at high energy ($270 < \lambda_{\text{irr}} < 290 \text{ nm}$) resulted in depletion of the band at 1936 cm^{-1} and those of the *endo* rotamer, and growth of the bands at 2131, 1866 and 1844 cm^{-1} . Careful wavelength-selective photolysis established that the *exo* rotamer was associated with the species with a single band at 1842 cm^{-1} , while the *endo* rotamer was associated with the species having a single band at 1866 cm^{-1} . Both of these new species were converted photochemically into the species with a single band at 1936 cm^{-1} . Upon annealing to ca. 133 K, the bands at 1866 and 1841 cm^{-1} decreased while the bands of the *endo* rotamer and the band at 1936 cm^{-1} grew in.

As found for **2**, long wavelength photolysis of **3** results in conversion of the *endo* rotamer to the *exo* rotamer, while photolysis at higher energy of a sample enriched in the *exo* isomer reforms the *endo* isomer. For **3**, photolysis at slightly higher energy is also found to stimulate carbon monoxide loss with the *endo* rotamer giving rise to a monocarbonyl species with an IR band at 1866 cm^{-1} and the *exo* rotamer producing a similar species with an IR band at 1844 cm^{-1} . Both monocarbonyl species give rise to a third monocarbonyl species with a single band 1936 cm^{-1} . We propose that the species initially formed by CO loss are the *endo* and *exo* isomers of $[\text{Mo}(\text{CO})(\eta^5\text{-C}_5\text{H}_5)(\eta^3\text{-C}_4\text{H}_7)]$ in which the orientation of the allyl group is retained. These species in turn undergo oxidative addition of the electron-deficient molybdenum into a C–H bond of the 2-methyl group to yield a trimethylenemethane ligand. The resulting compound, $[\text{Mo}(\text{CO})(\text{H})(\eta^5\text{-C}_5\text{H}_5)(\eta^4\text{-C}_4\text{H}_6)]$, would be analogous to $[\text{Mo}(\text{CO})(\text{CH}_3)(\eta^5\text{-C}_5\text{Me}_5)(\eta^4\text{-C}_4\text{H}_6)]$ for which the carbon monoxide stretching frequency is reported to be

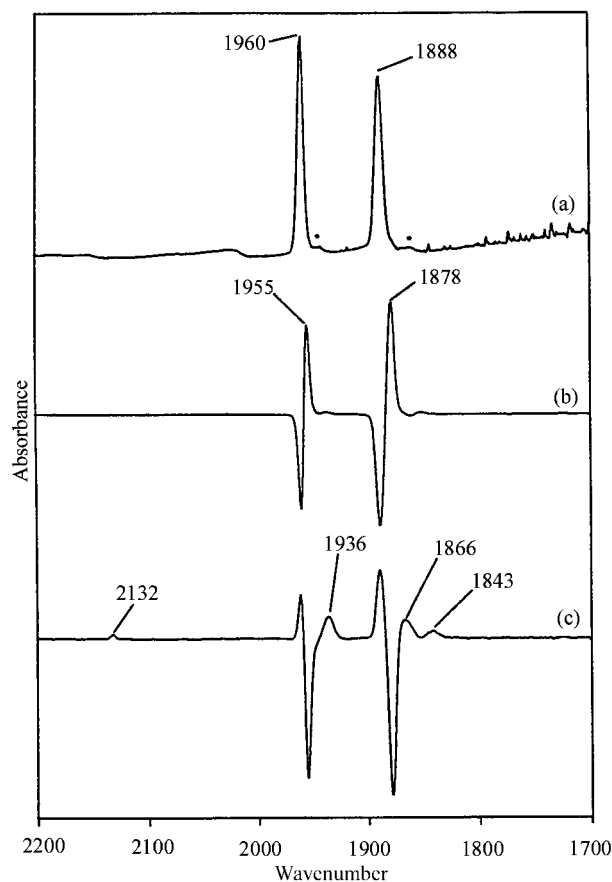
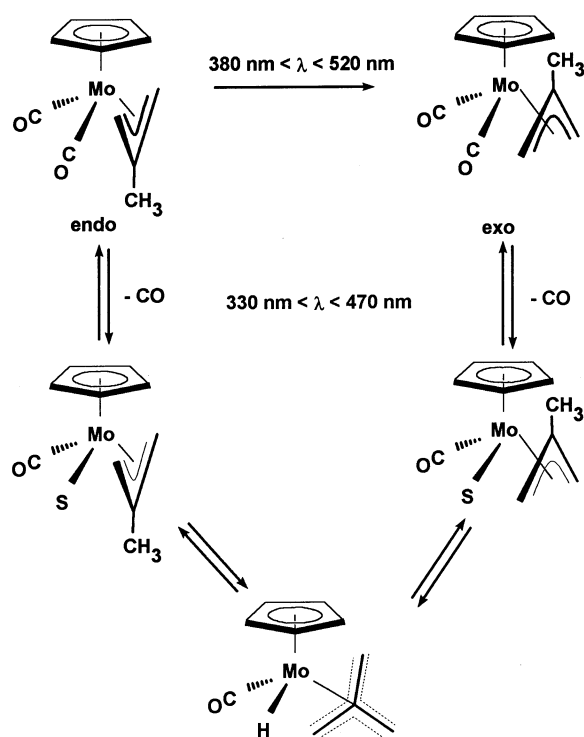


Figure 5. IR spectra of **3** isolated in a Nujol matrix: (a) starting material, ca. 90 K; (b) difference spectrum, 30 min. irradiation ($380 \text{ nm} < \lambda < 520 \text{ nm}$) minus starting material; (c) difference spectrum, 30 min. irradiation ($330 \text{ nm} < \lambda < 470 \text{ nm}$) minus 60 min. irradiation ($380 \text{ nm} < \lambda < 520 \text{ nm}$); the bands marked with an asterisk arise from natural abundance ^{13}CO

1925 cm^{-1} .^[11] We have reported a similar hydride shift in the photolysis of $[\text{Mo}(\text{CO})_2\{\eta^5, \eta^3\text{-C}_5\text{H}_4\text{C}(\text{CH}_3)_2\text{C}_5\text{H}_6\}]$ giving a species believed to be $[\text{Mo}(\text{CO})_2(\text{H})\{\eta^5, \eta^4\text{-C}_5\text{H}_4\text{C}(\text{CH}_3)_2\text{C}_5\text{H}_5\}]$ with a carbonyl band at 1917 cm^{-1} .^[12] These reactions are functionally identical to a beta-hydride transfer such as those observed by Rest for $[\text{M}(\text{CO})_3(\text{C}_2\text{H}_5)(\eta^5\text{-C}_5\text{H}_5)]$, where $\text{M} = \text{Mo}$ or W .^[13] Upon photolysis both the 16-electron intermediate $[\text{M}(\text{CO})_2(\text{C}_2\text{H}_5)(\eta^5\text{-C}_5\text{H}_5)]$ and the ethene, hydride species $[\text{M}(\text{CO})_2(\text{H})(\eta^2\text{-C}_2\text{H}_4)(\eta^5\text{-C}_5\text{H}_5)]$, were observed. Metal hydride bands are often weak, thus our inability to locate such a band in these spectra is not surprising. A summary of the proposed photochemical transformations for **3** is presented in Scheme 2.

Time-Resolved IR Studies

In order to further clarify the intermediates in these processes, time-resolved IR (TRIR) photochemical studies of **2** in *n*-heptane were carried out at room temperature. A 355 nm laser flash was employed to initiate the chemistry. Flash photolysis at this energy results in both CO loss to form the solvated intermediate $[(\eta^5\text{-C}_5\text{H}_5)\text{Mo}(\text{CO})(n\text{-heptane})(\eta^3\text{-C}_3\text{H}_5)]$, which has a single IR band at 1851 cm^{-1} ,



Scheme 2. Proposed photochemical transformations of $[(\eta^5\text{-C}_5\text{H}_5)\text{Mo}(\text{CO})_2(\eta^3\text{-C}_3\text{H}_4\text{CH}_3)]$

and *endo* to *exo* photoisomerization. The observed IR band at 1851 cm^{-1} is completely consistent with our observation of the equivalent Nujol-solvated species at 1842 cm^{-1} . The rate of reaction of $[(\eta^5\text{-C}_5\text{H}_5)\text{Mo}(\text{CO})(n\text{-heptane})(\eta^3\text{-C}_3\text{H}_5)]$ with CO was linear with [CO] and a second order rate constant, $k_2 = 1.5 \times 10^7 \text{ M}^{-1}\text{s}^{-1}$, was obtained.

Photoisomerization of the *endo* rotamer to the *exo* rotamer under argon was observed. The *exo* species decays, with $k_{\text{obs}} = 2 \times 10^5 \text{ s}^{-1}$, but does not appear to reform the *endo* species. The fate of this species is not clear at this time and additional work will be performed to clarify these observations.

Supercritical Ethene Studies

Compound **2** was found to be soluble in supercritical ethylene at 170 atm. and 40°C with approximately equal concentrations of the *endo* and *exo* rotamers. Photolysis of this solution with an unfiltered high pressure Hg/Xe lamp (45 min.) resulted in bleaching of the bands associated with **2** and growth of a new band at 1918 cm^{-1} . A small band at 2032 cm^{-1} attributable to free CO was also observed. It is believed that the species being formed in this case is $[(\eta^5\text{-C}_5\text{H}_5)\text{Mo}(\text{CO})(\eta^2\text{-ethene})(\eta^3\text{-C}_3\text{H}_5)]$. No effort was made to recover this compound.

Discussion

An explanation of the photochemistry of **2** and **3** must take into account the observed wavelength dependence of the *endo* to *exo* transformation. It is reasonable to postulate the existence of two distinct photochemical mechanisms,

one operating at low energy ($\lambda_{\text{irr}} > 400 \text{ nm}$) and a second at higher energy ($\lambda_{\text{irr}} < 400 \text{ nm}$). The high-energy transformation may have its origins in the same excited state responsible for CO loss.

Molecular orbital analyses of $[(\eta^5\text{-C}_5\text{H}_5)\text{Mo}(\text{CO})_2(\eta^3\text{-C}_3\text{H}_5)]$ have been conducted by Hoffmann^[14,15] and Rosenblum^[16] and their co-workers. The relevant molecular orbitals are illustrated in Figure 6. The allyl π orbital interacts with the s and p_z orbitals of the metal fragment, while the non-bonding allyl orbital (n) interacts with the a'' level. The metal-based orbitals $1a'$ and $2a'$ are effectively non-bonding and are the highest occupied molecular orbitals, while the LUMO is the antibonding combination of the n allyl orbital and the a'' ($a'' - n$). The MO analysis is supported by ultraviolet photoelectron spectral studies,^[17] in which the six observed bands were assigned to: I_1 and I_2 (metal d orbitals, $1a'$ and $2a'$), I_3 (allyl π HOMO, $n + a''$), I_4 and I_5 (cyclopentadienyl orbitals) and I_6 (second allyl π orbital, $\pi + s + p_z$).

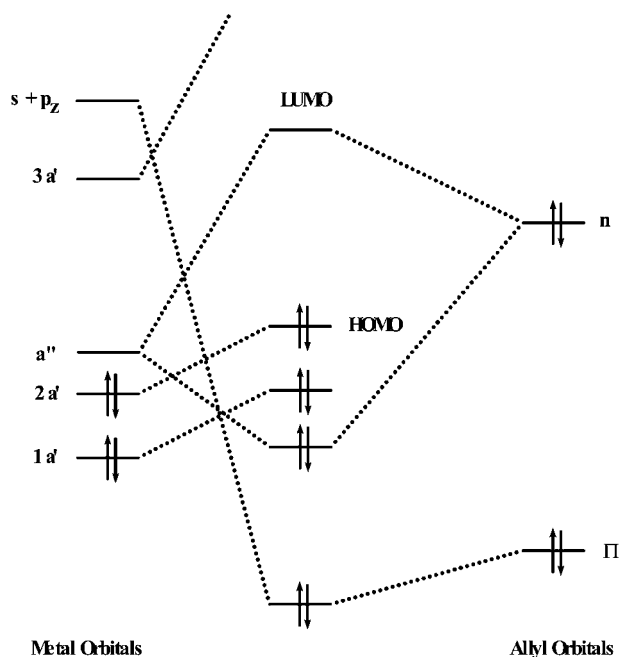


Figure 6. Molecular Orbital diagram for $[(\eta^5\text{-C}_5\text{H}_5)\text{Mo}(\text{CO})_2(\eta^3\text{-C}_3\text{H}_5)]$ based on the previous work of Hoffmann^[11,12] and Rosenblum^[13]

Hoffmann has argued that *endo* to *exo* exchange observed by NMR spectroscopy should not involve simple rotation of the allyl fragment since such a rotation brings the allyl non-bonding orbitals into an orientation where the bonding with the metal is lost. However, the photochemical promotion of a $1a'$ or $2a'$ d electron to the LUMO level weakens this interaction permitting rotation about the symmetric allyl π – metal ($\pi + s + p_z$) orbital. Such a process is functionally identical to that which results in *cis* to *trans* olefin photoisomerization in organic chemistry. We assign the shoulder at 400 nm to the $1a'$, $2a' \rightarrow a'' - n$ transition. The band at 345 nm is assigned to the $d \rightarrow d$ transition ($1a'$, $2a' \rightarrow 3a'$), while higher energy bands are assigned to

metal-to-ligand charge transfers. The wavelength selectivity of the filters used in this study are not sufficiently narrow to distinguish with certainty whether the excitations leading to *exo* to *endo* transformations and carbonyl loss are associated with the band at 345 nm or with the tails of the higher energy bands.

The mechanism of the higher energy *exo* to *endo* transformations is not entirely clear. The concurrent appearance of species formed by CO loss indicates that sufficient energy may be available for an $\eta^3 \rightarrow \eta^1 \rightarrow \eta^3$ sequence, even though no η^1 species was observed in either Nujol or in the donor solvent MeTHF. We have, however, observed an analogous transformation in the case of $[\text{Mo}(\text{CO})_2\{\eta^5, \eta^3\text{-C}_5\text{H}_4\text{-C}(\text{CH}_3)_2\text{-C}_5\text{H}_6\}]$ in which a pendant cyclopentenyl group is connected to the cyclopentadienyl ring by an isopropyl link. Matrix isolation studies have established that low energy photolysis results in an $\eta^3 \rightarrow \eta^1$ opening, and higher energy photolysis results in loss of CO. The comparative ease in stimulating the hapticity change in the case of this pendant allyl is attributed to the relief of strain in the open form.^[5]

Our work and that of Limberg et al.^[7] require a reinterpretation of the observations reported by Rest et al.^[6] on the gas matrix photolysis of $[\text{W}(\eta^5\text{-C}_5\text{H}_5)(\text{CO})_3(\eta^1\text{-C}_3\text{H}_5)]$. These workers observed loss of CO and the appearance of four bands attributable to metal carbonyl species. Continued photolysis resulted in the decrease of one pair of these new bands and growth of the second pair. Reexamination of the reported spectra in light of the present work strongly suggest that the four bands that arise upon photolysis are due to the *endo* and *exo* rotamers of $[\text{W}(\eta^5\text{-C}_5\text{H}_5)(\text{CO})_2(\eta^3\text{-C}_3\text{H}_5)]$, and that the subsequent growth of one pair of these bands at the expense of the second is identical to the behavior of the molybdenum analogue reported herein.

Experimental Section

Compounds **1**, **2**, and **3** were prepared by standard literature procedures.^[8]

Nujol matrix studies were carried out using a glass cryostat designed by Dr. A. J. Rest of the University of Southampton (UK). This apparatus and experimental procedures have been described previously.^[9] Nujol solutions were prepared by dissolving 1–2 mg of sample in Nujol at room temperature. All samples were centrifuged to remove particulates and eliminate the possibility of having microcrystals in the photolysis sample. MTHF glass matrices were carried out using a Specac Model 21525 variable temperature cell with a sample temperature of ca. 90 K.

Photolyses were carried out at ca. 90 K using a 350 watt high pressure mercury lamp. A water filter was used to remove IR radiation from the beam and optical filters were used to carry out wavelength selective photochemistry. In some cases, the photolyzed sample was annealed to permit the Nujol glass to soften and allow either recombination or rearrangement reactions. The temperature of the sample during the annealing steps was monitored by a thermo-

couple mounted on the sample cell. All spectra are recorded at 4 cm^{-1} resolution.

Time-resolved IR studies were carried out at the University of Nottingham employing a pulsed Nd:YAG laser (Quanta-Ray GCR-12, ca. 7 ns, 355 nm) to initiate photochemical reactions. A continuous wave IR diode laser (Mütek MDS 1100) was used to monitor the transient IR absorptions. Details of the apparatus and procedures have been reported.^[18]

Photolyses in supercritical ethene were conducted using a high pressure cell with diamond IR windows and a sapphire window for photolysis. Photolyses were carried out using a high pressure Hg/Xe lamp.

Acknowledgments

This work was supported by the Research Corporation and the Director, Office of Science, Office of Basic Energy Sciences, Chemical Sciences Division of the U. S. Department of Energy under contract DE-AC0676RLO 1830.

- [1] M. Cousins, M. L. H. Green, *J. Chem. Soc.* **1963**, 889–894.
- [2] R. B. King, *Inorg. Chem.* **1966**, 5, 2242–2243.
- [3] A. Davidson, W. C. Rode, *Inorg. Chem.* **1967**, 6, 2124–2125.
- [4] [4a] J. W. Faller, M. J. Incorvia, *Inorg. Chem.* **1968**, 7, 840–842. — [4b] J. W. Faller, A. J. Jakubowski, *J. Organomet. Chem.* **1971**, 31, C75–C78. — [4c] J. W. Faller, D. F. Chodosh, D. J. Katshira, *J. Organomet. Chem.* **1980**, 187, 227–231.
- [5] T. E. Bitterwolf, A. A. Saygh, J. T. Bays, B. Scallorn, C. Weiss, A. L. Rheingold, L. Liable-Sands, J. E. Shade, *J. Organomet. Chem.* **1999**, 583, 152–161.
- [6] R. B. Hitam, K. A. Mahmoud, A. J. Rest, *J. Organomet. Chem.* **1985**, 291, 321–333.
- [7] C. Limberg, A. J. Downs, T. M. Greene, T. Wistuba, *Eur. J. Inorg. Chem.* **2001**, 2613–2618, preceding paper.
- [8] [8a] D. H. Gibson, W.-L. Hsu, D.-S. Lin, *J. Organomet. Chem.* **1979**, 172, C7–C12. — [8b] R. G. Hayter, *J. Organomet. Chem.* **1968**, 13, 1–3. — [8c] W. E. Vanarsdale, J. K. Kochi, *J. Organomet. Chem.* **1986**, 317, 215–232.
- [9] T. E. Bitterwolf, K. A. Lott, A. J. Rest, J. Mascetti, *J. Organomet. Chem.* **1991**, 419, 113–126.
- [10] A. J. Rest, D. J. Taylor, *J. Chem. Soc., Dalton Trans.* **1983**, 1291–1298.
- [11] C. G. Kreiter, G. Wendt, W. S. Sheldrick, *J. Organomet. Chem.* **1987**, 333, 47–59.
- [12] T. E. Bitterwolf, A. A. Saygh, J. T. Bays, C. A. Weiss, W. B. Scallorn, J. E. Shade, A. L. Rheingold, L. Liable-Sands, *J. Organomet. Chem.* **1999**, 583, 152–161.
- [13] [13a] K. A. Mahmoud, A. J. Rest, H. G. Alt, M. E. Eichner, B. M. Jansen, *J. Chem. Soc., Dalton Trans.* **1984**, 175–186. — [13b] R. J. Kazlauskas, M. S. Wrighton, *J. Am. Chem. Soc.* **1982**, 104, 6005–6015. — [13c] R. J. Kazlauskas, M. S. Wrighton, *J. Am. Chem. Soc.* **1980**, 102, 1727–1730.
- [14] B. E. R. Schilling, R. Hoffmann, J. W. Faller, *J. Am. Chem. Soc.* **1979**, 101, 592–598.
- [15] B. E. R. Schilling, R. Hoffmann, D. L. Lichtenberger, *J. Am. Chem. Soc.* **1979**, 101, 585–591.
- [16] R. W. Fish, W. P. Giering, D. Marten, M. Rosenblum, *J. Organomet. Chem.* **1976**, 105, 101–118.
- [17] S. D. Worley, D. H. Gibson, W.-L. Hsu, *Inorg. Chem.* **1981**, 20, 1327–1328.
- [18] M. W. George, M. Poliakoff, J. J. Turner, *Analyst* **1994**, 551–560.

Received February 28, 2001

[I01073]